Journal of Ceramic Processing Research. Vol. 2, No. 1, pp. 21~26 (2001)

J O U R N A L O F
Ceramic Processing Research

The synthesis and thermal behavior of a heterometallic molecular precursor for lithium niobate

Seung Kju Park, Jung Woo Park and Sang Man Koo*

Department of Chemical Engineering and Ceramic Processing Research Center, College of Engineering, Hanyang University, Seoul 133-791, Korea

The metathesis reactions of $NbCl_5$ with lithium 2,6-dimethylphenoxide (LiO-2,6-$PhMe_2$) afforded $LiNbO(O\text{-}2,6\text{-}PhMe_2)_4$ 3THF which has been characterized by FT-IR, NMR and single crystal X-ray analysis. This molecular precursor was converted into pure $LiNbO_3$ after heat treatment. Thermal conversion of this precursor can be divided into two stages: 1) at low calcinations temperature (200-400°C), where the progressive formation (crystallization) of $LiNbO_3$ was observed; 2) at high calcinations temperature (600-1000 °C), where grain growth and secondary crystallization occurred. From the FT-IR/XRD/ TG-DTA investigations, it was found that the crystallization temperature of $LiNbO_3$ for the current precursor system is significantly lower than those for conventional precursor systems.

Key words: molecular precursor, lithium niobate, hetereometallic precursor.

Introduction

Nowadays heterometallic oxides of high purity are of considerable importance in the development of high-tech ceramic materials [1, 2]. In particular, lithium niobate ($LiNbO_3$, LN) single crystal is an excellent material for electro-optic and nonlinear optic devices, such as optical wave-guides, surface acoustic wave devices, holographic memories, etc. [3-15]. With the development of processes, demand for molecularly - defined precursors has increased [16-32]. As an effort to search for new routes of $LiNbO_3$ synthesis, there has been an enormous emphasis on the preparation of heterometallic lithium niobium alkoxides in recent years. Heterometallic lithium niobium alkoxides with the desired stoichiometry of the lithium and niobium are extremely attractive single-source precursors to fabricate $LiNbO_3$ due to their significant advantages in the composition control of final ceramic materials and simplification in processings [16-32]. However, the chemistry of lithium niobium alkoxides remains relatively un-explored. Since the first report for the syntheses of lithium niobium (V) alkoxides, $[LiNb(OR)_6]_x$ (R=Me, Et, *i*Pr, *t*Bu) [29], a few complexes have been synthesized and characterized: $[LiNb(OEt)_6]_x$ of helical structure [30] and $[LiNbO(OEt)_4\ EtOH]_2$ [16, 25, 31] as an intermediate in the hydrolysis reaction to $[LiNb(OEt)_6]_x$. More recently, $[LiNb(OR)_6]_2$ (R=CH_2CMe_3, CH_2SiMe_3), dimeric molecular precursors, have been prepared and characterized [32] Our motivation for exploring lithium niobium alkoxides concerns the development of improved molecular singlesource precursors for $LiNbO_3$. To obtain molecular lithium niobium complexes without any intermolecular bonds or bridging units, we have introduced aryl- and bulky aryl-compound containing methyl side chains as organic groups [33]. This study reports the syntheses and structural characterizations of the first examples of a monomeric lithium niobium (V) oxo aryl-alkoxide, $LiNbO(O\text{-}2,6\text{-}PhMe_2)_4 \cdot 3THF$, which may be an intermediate in hydrolysis and/or condensation reactions of lithium niobium phenoxide. To estimate the application of a complex as a molecular precursor for fabrication of $LiNbO_3$, we have investigated thermal behavior of this complex, and the quality of the final ceramic material has been established throughout FT-IR, TG/DTA, XRD, and SEM methods. The possible mechanism of the conversion from precursor to $LiNbO_3$ ceramic material has also been proposed.

*Corresponding author:
Tel : +82-2-2290-0527
Fax: +82-2-2281-4800
E-mail: sangman@hanyang.ac.kr

Experimental

Syntheses of Precursors

All reactions and manipulations were carried out under dry inert gas using a standard Schlenk line technique. Solvents were dried and purified by distillation from sodium benzophenone ketyl under nitrogen. Niobium chloride (Strem Chemicals), lithium (Aldrich Chemical Co.), and 2,6-dimethylphenol (Aldrich Chemical Co.) were used in their as received states. Lithium-2,6-dimethyl-phenoxide was prepared from metallic lithium and 2,6-dimethylphenol in diethyl ether. FT-IR spectra were obtained using the KBr pellet technique on a Nicolet Magna-IR 760 spectrometer. NMR spectra were registered on a Varian Gemini 300 spectrometer. Analytical data

were obtained with a Thermoquest EA-1110 CHNS analyzer.

Synthesis of LiNbO(O-2,6-PhMe$_2$)$_4$ · 3THF

A solution of $NbCl_5$ (2 g, 7.4 mmol) in THF (50 ml) was added dropwise to a solution of 6 equivalent LiO-2,6-PhMe$_2$ (5.7 g, 44.5 mmol) in THF (50 ml). The resultant mixture was stirred at ambient temperature for 24 h. After the removal of THF solvent, diethyl ether (150 ml) was added, and the mixture was filtered to eliminate LiCl. After concentration to half volume, THF (50 ml) was added and the solution was layered with *n*-hexane. Complex **1** was obtained as yellow crystals with 72% (4.35 g) yield. Analysis found: C, 64.74; H, 7.67. Calculation for $C_{44}H_{60}O_8LiNb$: C, 64.70; H, 7.40. FT-IR (cm^{-1}, KBr): 3010(w), 2976(m), 2880(m), 1594(w), 1467(s), 1426(s), 1372(w), 1273(vs), 1225(vs), 1088(m), 1048(m), 918(m), 880(s), 754(s), 737(m), 713(s), 566(m), 546(m). ^{1}H NMR ($CDCl_3$, 25°C, ppm): 6.94-6.51 (m, 12H, OC$_6$*H*$_3$Me$_2$); 3.66 (t, 12H, OC*H*$_2$CH$_2$); 2.15 (s, 24H, OC$_6$H$_3$*Me*$_2$); 1.76 (quintet, 12H, OCH$_2$C*H*$_2$). ^{13}C {^{1}H} NMR ($CDCl_3$, 25°C, ppm): 160.5, 128.5, 127.8, 127.2, 123.5, 121.1, 119.6, 118.9 (O*C*$_6$H$_5$Me$_2$); 68.2 (O*C*H$_2$CH$_2$); 25.4 (OCH$_2$*C*H$_2$); 17.0, 16.2 (OC$_6$H$_5$*Me*$_2$).

Crystallography of LiNbO(O-2,6-PhMe$_2$)$_4$ · 3THF

Single crystals suitable for X-ray diffraction study were grown from THF and *n*-hexane for a complex. A suitable crystal was mounted inside a glass capillary under a nitrogen atmosphere and sealed with a flame. Diffraction data were collected on a Bruker P4 four circle instrument, with graphite-monochromated Mo-Kα radiation (λ=0.71073). The unit cell parameters and basic information about data collection and structural refinement are given in Table 1. The solutions of the structures were carried out by a combination of heavy atom Patterson technique, a direct method, and Fourier techniques with SHELXS-86 and refined against F^2 on all data by full matrix least-squares with SHELXL-93. All non-hydrogen atoms were refined anisotropically. Hydrogen atoms were included at geometrically calculated positions and refined using a riding model.

Thermal behavior of precursor: LiNbO(O-2,6-PhMe$_2$)$_4$ · 3THF

The precursor was calcined at different temperatures and times in a tubular furnace: (a) at 200, 300, 400, 500, and 600°C for 3 h, (b) at 600, 800, and 1000°C for 3, 6, and 12 h. The calcination was performed at a heating rate of 10°C/min with static air. These heat-treated precursors were grown as micro-sized particles after calcination. The nomenclature of the resulting samples are expressed in the text as P200, P300, P400 and so on.

The chemical composition and evolution of chemical species in the calcined precursors were examined with an FT-IR spectroscopic method (the KBr pellet technique). The FT-IR spectra of the samples were recorded with a 4 cm^{-1} resolution in a dry environment (Nicolet Magna-IR 760 spectrometer). The crystallographic information on the calcined precursors were established using an X-ray diffraction (XRD) method. The diffraction intensity were measured in a Rigaku Rint2000 with Cu Kα radiation (λ=1.54056Å) with a 2θ range of 5~90° at a scanning rate of 5°/min. The thermal behavior of the precursor was also studied with the thermogravimetric/differential thermal analysis (TG/DTA). The TG/DTA measurements were performed on a TA Instruments SDT 2960 in an air atmosphere with a gas flow rate of 60 ml/min. The temperature was scanned from room temperature to 1400°C at a heating rate 10°C/min. The microstructure and morphology of the calcined precursors were examined on a JEOL JSM-6340F scanning electron

Table 1. Crystal data for LiNbO(O-2,6-PhMe$_2$)$_4$ · 3THF

Complex	**1**		
Formula	$C_{44}H_{60}O_8LiNb$	Scan type	θ/2θ
FW	816.77	θ range (°)	1.83 ≤ θ ≤ 22.52
Crystal system	Monoclinic	Index ranges	-14.0; -22.0; -17.17
Space group	$P2_1/n$	*F* (000)	1728
A (Å)	13.226(1)	Rflt. Collected	6149
b (Å)	20.709(2)	Indpt. Collected	5877
c (Å)	16.559(2)	*R* (int)	0.1737
β (°)	90.54(1)	R_1[a]	0.0673(0.0889)
V (Å^3)	4535.3(8)	WR_2[b]	0.2030(0.2418)
Z	4	GOF[c]	1.028
ρ_{calcd} (gcm^{-3})	1.196	$\Delta\rho$ (e^{-3})	-0.707/0.575
μ (mm^{-1})	0.312	No. of variables	547
Temperature (K)	293(2)		

[a] $R_1 = \Sigma||F_o|-|F_c||/\Sigma|F_o|$
[b] $wR_2 = [\Sigma w(F^2_o-F^2_c)^2/\Sigma wF^4_o]^{1/2}$ for data with $I>2\sigma(I)$
[c] GOF = $[\Sigma w(F^2_o-F^2_c)^2/\Sigma(n-p)]^{1/2}$

microscope (SEM).

Results and Discussion

Synthesis and Characterization

The metathesis reaction of niobium chloride, $NbCl_5$, with lithium-2,6-dimethylphenoxide, LiO-2,6-$PhMe_2$, was investigated in THF at room temperature. A complex of formula $LiNbO(O\text{-}2,6\text{-}PhMe_2)_4 \cdot 3THF$ was obtained by adding a THF solution of $NbCl_5$ to a THF solution of 6 equivalent LiO-2,6-$PhMe_2$. The FT-IR spectra exhibit stretching modes, ν (COC) from coordinated THF molecules at 1048 (m) and 880 cm^{-1} (s) and a sharp band at 918 cm^{-1} (m) from ν (Nb=O), which is shifted to lower frequencies compared to ν (Nb=O), 962 cm^{-1} of $[NbOCl_4(THF)]^-$ anion [34] The bands at 566 (m) and 546 cm^{-1} (m) are assigned to ν (NbO) vibrations from arylalkoxide ligands [35] ^1H and $^{13}C\{^1H\}$ NMR spectra of complex in $CDCl_3$ show two types of resonance for 2,6-dimethylphenoxy ligands. The presence of two types of resonance suggests the magnetic non-equivalent surroundings for 2,6-dimethylphenoxy ligands. The molecular structure was determined by X-ray single crystal diffraction analysis. The ORTEP diagram of complex is presented in Fig. 1.

The molecular structure of the complex includes niobium square pyramid and lithium tetrahedron units. The niobium is five-coordinated by a terminal oxo ligand in an axial position and four 2,6-dimethylphenoxy ligands in the basal plane of a square pyramid. The lithium is four-coordinated by three oxygen atoms of the THF molecules and the terminal oxo ligand in the $[NbO(O\text{-}2,6\text{-}PhMe_2)_4]^-$ unit.

Chemical and Physical Changes of the Precursor Under Conversion to the Ceramic $LiNbO_3$

The chemical composition and evolution of chemical species in the precursor and the calcined precursors were investigated with FT-IR spectroscopy. The FT-IR spectra for the precursor and the calcined products at different temperatures are presented in Fig. 2. For low-temperature calcined samples P200-P300, the absorption band at 1470 cm^{-1} is assigned to C=C aromatic stretching of the 2,6-dimethylphenoxy ligands. The broad absorption bands located in the range 1430~1380 cm^{-1} are due to CH_3, asymmetric bending (1430 cm^{-1}) and CH_2 symmetric bending (1380 cm^{-1}), respectively. For P200, the C-O stretching vibration of O-2,6-$PhMe_2$ at 1270 cm^{-1} can be clearly identified. These hydrocarbon species reflect the fact that organic components still remained in the low temperature (200~300°C) calcined precursors. When the calcination temperature is increased to 500°C, absorption peaks due to organic groups disappear (P500, Fig. 2), suggesting that the decomposition of the organic moiety occurs below this temperature.

The TG/DTA analyses (Fig. 3) is also in good agreement with the FT-IR results. The endothermic peaks below 240°C are attributed to the evaporation of the coordinated THF molecules in the lithium atom. However, combining the TG/DTA result with that of

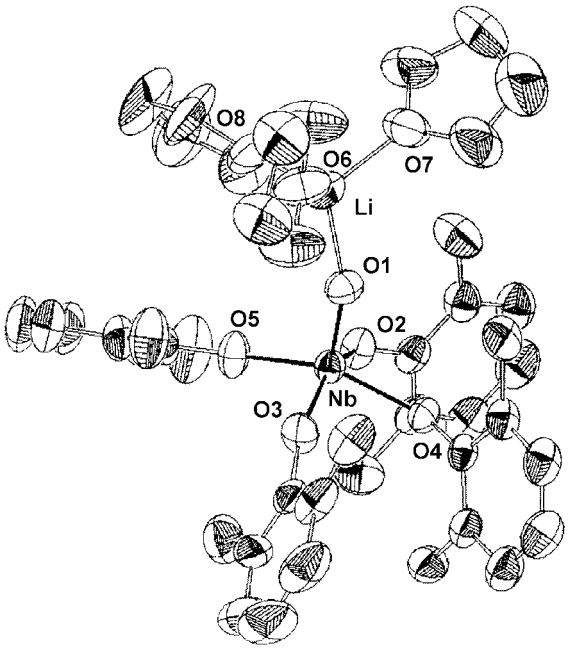

Fig. 1. ORTEP diagram of $LiNbO(O\text{-}2,6\text{-}PhMe_2)_4 \cdot 3THF$ (**1**) in the solid state. The hydrogen atoms are omitted for clarity. (Nb-O1:1.730(5); Nb-O2: Nb-O2:1.948(4), Nb-O3:1.940(5); Nb-O4: 1.985(4); Nb-O5:1.922(5); Li-O1:1.88(2); Li-O6:1,95(2); Li-O7:1.96(2); Li-O8:1.90(2)).

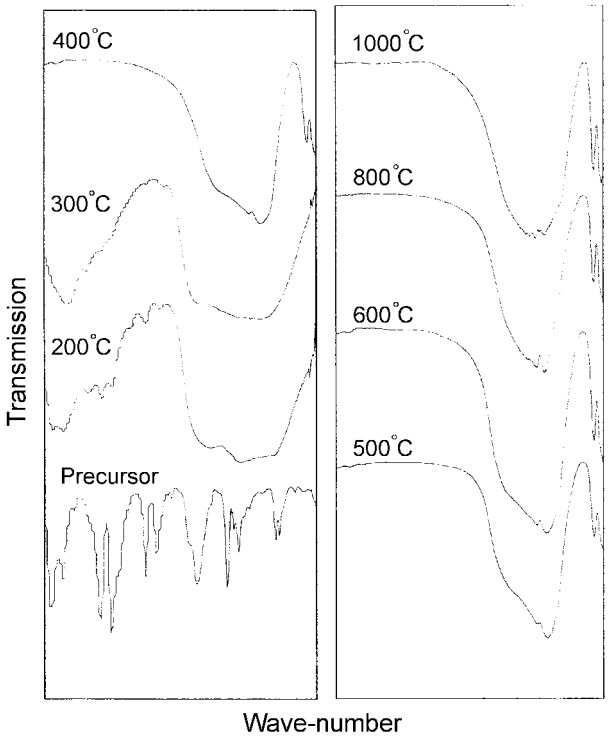

Fig. 2. FT-IR spectra for $LiNbO(O\text{-}2,6\text{-}PhMe_2)_4 \cdot 3THF$ (**1**) and the calcined precursors (200-1000°C).

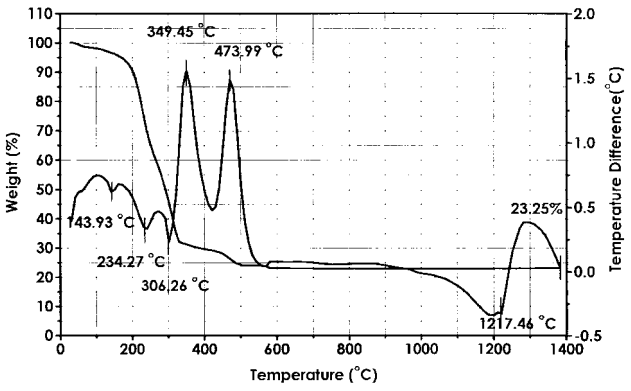

Fig. 3. TG/DTA analysis for $LiNbO(O\text{-}2,6\text{-}PhMe_2)_4 \cdot 3THF$ (**1**) from room temperature to 1400°C, measured at 10°C/min in air atmosphere with a flow rate of 60.0 ml/min.

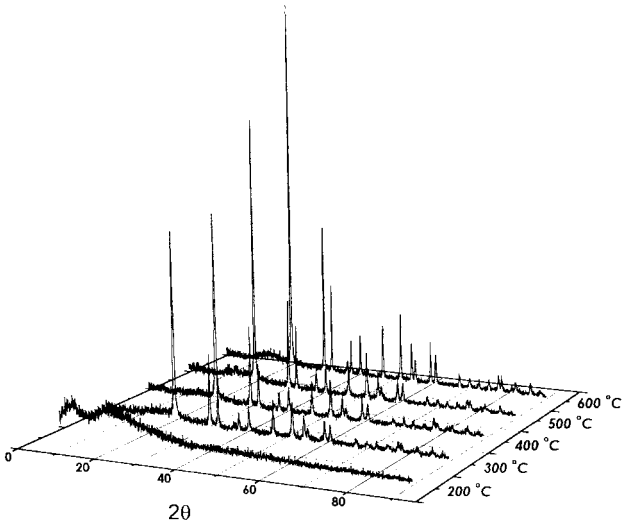

Fig. 4. XRD spectra for the low-temperature calcined precursors for 3 h (200~600°C).

FT-IR analysis, it is clear that there are actually several stages involved in this process. The coordinated THF molecules are evaporated step-by-step. The evaporation of the first THF molecule takes place at a temperature below 100°C and those of the second and the third THF molecules take place subsequently at 144 and 234°C. The three sharp endothermic bands in this temperature range in the TG/DTA result and the C-O stretching mode of THF at 1220 cm^{-1} in the FT-IR spectrum of P200 support this fact, while the C-O stretching mode of THF at 1220 cm^{-1} cannot be observed in P300. The evaporation processes separated as three steps can be explained by the weak interaction between the coordinated THF molecules and the lithium atom. The doublet peaks at 349 and 473°C in TG/DTA spectrum can be assigned to the combustion of organic residues, 2,6-dimethylphenoxy ligands ($O\text{-}2,6\text{-}PhMe_2$), since the FT-IR result shows absorption peaks from these functional groups disappear over this temperature range. Accompanied with the decomposition of organic groups, the formation of $LiNbO_3$ can be clearly observed in the range of 400~800 cm^{-1} in the FT-IR spectrum of P400. After the calcination over 500°C, the precursor is converted to $LiNbO_3$, which are not contaminated by any retained organic components.

Crystallization of the Calcined Precursors

In the precursor, the formation of a Li-O-Nb framework is supported by the fact that the characteristic $LiNbO_3$ FT-IR finger printing absorption bands over the range of 400~800 cm^{-1} which are observed for the precursor, P200, although the XRD pattern reveals the calcined material is still amorphous over this temperature. These absorption modes are getting more pronounced when the temperature is increased to 400°C. In Fig. 4, the XRD results are shown for five low-temperature calcined precursors, P200-P600. As can be seen from the XRD spectrum of P300, the characteristic diffraction features for $LiNbO_3$ are observed at a low calcination temperature (300°C). However, conversion from the amorphous precursor to the single phase crystalline $LiNbO_3$ is completed above the calcination at 500°C for 3 h.

In agreement with the above FT-IR/XRD observations, TG/DTA data in Fig. 3 shows the formation of $LiNbO_3$ from the precursor during the thermal process. The endothermic peak at 1217°C corresponds to the melting point (the liquids temperature) of this *on-site* synthesized $LiNbO_3$ (Li_2O: m.p. 1570°C; Nb_2O_5: m.p. 1520°C). The melting point presented in the TG/DTA analysis indicates that the calcined precursor maintains well its chemical composition of $LiNbO_3$.

Microstructural Evolution of $LiNbO_3$ Powder

The morphologies and the microstructures of the high temperature calcined $LiNbO_3$ ceramics for 3 h, 6 h, and 12 h were determined in a scanning electron microscope (SEM). As shown in Fig. 5, the high temperature calcined $LiNbO_3$ powder shows "ball-like" structures. After heat treatment at 600°C for 3 h, the calcined precursor grows as fine crystalline grains of 40~50 nm (Fig. 5(a)). When the precursor is calcined at the higher temperature, grain growth becomes more apparent.

In order to investigate grain growth with at different calcination temperatures and times, XRD analyses were performed for heat treated product at different temperatures 3 h, 6 h, and 12 h (Fig. 6). As can be informed from Fig. 6, there is a sharp increase in the grain size at 1000°C. This sudden rise in the grain size can be described due to the secondary recrystallization, which refers to rapid grain growth at the expense of a fine-grained matrix in ceramic science. For example, it is evident that the average $LiNbO_3$ grain size of the P1000 (Fig. 5) is 5 μm, which is about 100 times greater than that of the P600, and the pore population is markedly reduced. With the calcination temperature of 1000°C, the $LiNbO_3$ particles are highly densified, and the morphologies of the particles change significantly

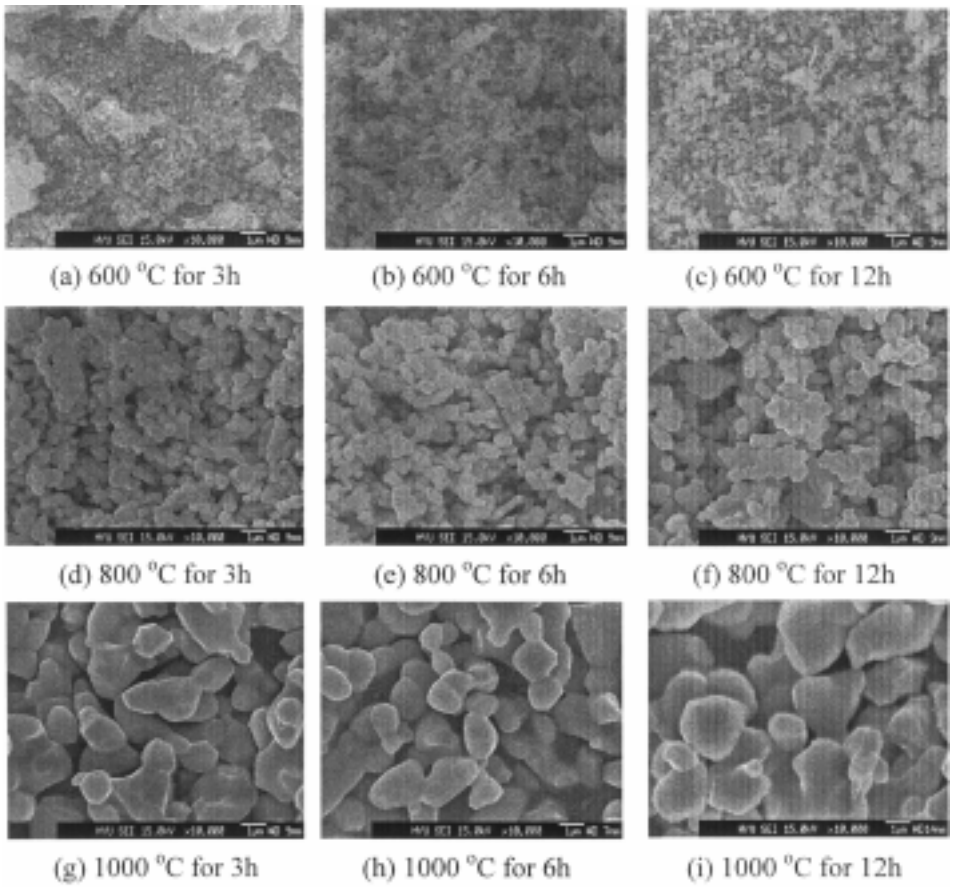

Fig. 5. SEM micrographs of the calcined $LiNbO_3$ powders at 600°C (a) for 3 h, (b) 6 h, (c) 12 h; at 800°C (d) for 3 h, (e) 6 h, (f) 12 h; at 1000°C (g) for 3 h, (h)n 6 h, and (i) 12 h. Bar lengths represent 1 μm.

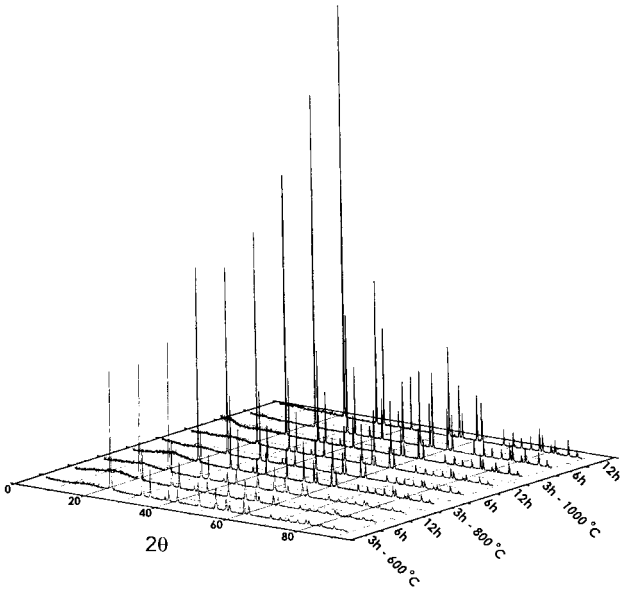

Fig. 6. XRD spectra for the high-temperature calcined precursors for 3 h, 6 h, and 12 h (600~1000°C).

(Fig. 5(i)). As can be seen from the micrograph of Fig. 5(i), the grain boundaries disappear in the P1000-12h. The calcination temperature rather than the time probably affects the crystallinity of the calcined precursor. The intensity in the XRD pattern for the high temperature calcinated precursors was enhanced with the increasing temperature.

Conclusions

A novel lithium niobium compound was obtained from the metathesis reactions of $NbCl_5$ with lithium 2,6-dimethylphenoxide (LiO-2,6-$PhMe_2$). LiNbO (O-2,6-$PhMe_2)_4 \cdot 3THF$ is used as a potential precursor for the fabrication of $LiNbO_3$. After heat treatment, the monomeric precursor, yielded pure $LiNbO_3$. The progressive formation (crystallization) of $LiNbO_3$ was observed over a low-calcination temperature ranges, 200~400°C. It was found that grain growth and secondary recrystallization occurred sequentially at high-temperatures. From the FT-IR/XRD/TG-DTA investigations, the crystallization temperature of $LiNbO_3$ for the current precursor system is significantly lower than those for conventional precursor systems.

References

1. D.C. Bradley, Chem. Rev. 89 (1989) 1317-1322.
2. L.G. Hubert-Pfalzgraf, Appl. Organomet. Chem. 6 (1992) 627-643.
3. J.R. Carruthers, G.E. Peterson, M. Grasso, P.M. Bridenbaugh,

J. Appl. Phys. 42 (1971) 1846-1851.
4. L.O. Svaasand, M. Eriksrud, G. Nakken, A.P. Grande, J. Cryst. Growth 22 (1974) 230-232.
5. P.K. Gallagher, H.M. O'Bryan, Jr., J. Am. Ceram. Soc. 68 (1985) 147-150.
6. H.M. O'Bryan, P.K. Gallagher, C.D. Brandle, J. Am. Ceram. Soc. 68 (1985) 493-496.
7. B. Guenais, M. Baudet, M. Minier, M. LeCun, Mater. Res. Bull. 16 (1981) 643-653.
8. P.K. Gallagher, H.M. O'Bryan, Jr., J. Am. Ceram. Soc. 71 (1988) C56-C59.
9. D.P. Birnie, III, J. Mater. Sci. 28 (1993) 302-315.
10. I. Baumann, P. Rudolph, D. Krabe, R. Schalge, J. Cryst. Growth 128 (1993) 903-908.
11. Y. Furukawa, M. Sato, K. Kitamura, F. Nitanda, J. Cryst. Growth 128 (1993) 909-914.
12. S. Kan, M. Sakamoto, Y. Okano, K. Hoshikawa, T. Fukuda, J. Cryst. Growth 128 (1993) 915-919.
13. T. Fukuda, H. Hirano, J. Cryst. Growth 50 (1980) 291-298.
14. B.S. Redkin, V.N. Kurlov, V.A. Tatarchenko, J. Cryst. Growth 82 (1987) 106-109.
15. Y.S. Luh, R.S. Feigelson, M.M. Fejer, R.L. Byer, J. Cryst. Growth 78 (1986) 135-143.
16. W.A. Herrmann, N.W. Huber, O. Runte, Angew. Chem. Int. Ed. Engl. 34 (1995) 2187-2206.
17. R.C. Mehrotra, A. Singh, Chem. Soc. Rev. (1996) 1-14.
18. K.G. Caulton, L.G. Hubert-Pfalzgraf, Chem. Rev. 90 (1990) 969-995.
19. C.D. Chandler, C. Roger, M.J. Hampden-Smith, Chem. Rev. 93 (1993) 1205-1241.
20. D. Segal, J. Mater. Chem. 7 (1997) 1297-1305.
21. D.C. Bradley, Polyhedron 13 (1994) 1111-1121.
22. L.G. Hubert-Pfalzgraf, Polyhedron 13 (1994) 1181-1195.
23. U. Schubert, J. Chem. Soc., Dalton Trans. (1996) 3343-3348.
24. T.J. Boyle, R.W. Schwartz, Comments Inorg. Chem. 16 (1994) 243-278.
25. E.P. Turevskaya, N.Y. Turova, A.V. Korolev, A.I. Yanovsky, Y.T. Struchkov, Polyhedron 14 (1995) 1531-1542.
26. R. Papiernik, L.G. Hubert-Pfalzgraf, J.C. Daran, Y. Jeannin, J. Chem. Soc., Chem. Commun. (1990) 695.
27. S. Boulmaâz, R. Papiernik, L.G. Hubert-Pfalzgraf, B. Septe, J. Vaissermann, J. Mater. Chem. 7 (1997) 2053-2061.
28. P. Sobota, J. Utko, S. Szafert, Inorg. Chem. 36 (1997) 2227-2229.
29. R.C. Mehrotra, M.M. Agrawal, P.N. Kapoor, J. Chem. Soc. A (1968) 2673-2676.
30. D.J. Eichorst, D.A. Payne, S.R. Wilson, K.E. Howard, Inorg. Chem. 29 (1990) 1458-1459.
31. A.I. Yanovsky, E.P. Turevskaya, N.Y. Turova, Y.T. Struchkov, Soviet J. Coord. Chem. 11 (1985) 63.
32. S.C. Goel, J.A. Hollingsworth, A.M. Beatty, K.D. Robinson, W.E. Buhro, Polyhedron 17 (1998) 781-790.
33. V.W. Day, T.A. Eberspacher, W.G. Klemperer, S. Liang, Chem. Mater. 7 (1995) 1607-1608.
34. H.C. Aspinall, M.M. Roberts, S.J. Lippard, Inorg. Chem. 23 (1984) 1782-1784.
35. K.C. Malhotra, U.K. Banerjee, S.C. Chaudhry, J. Indian Chem. Soc. 7L (1980) 868-870.